Available online at www.sciencedirect.com
SCIENCE DIRECT®
PERGAMON
International Journal of Heat and Mass Transfer 46 (2003) 3573–3582
International Journal of HEAT and MASS TRANSFER
www.elsevier.com/locate/ijhmt

Measurements in three-dimensional laminar separated flow

B.F. Armaly *, A. Li, J.H. Nie

Department of Mechanical and Aerospace Engineering, and Engineering Mechanics, University of Missouri—Rolla, Rolla, MO 65401, USA

Received 13 December 2002; received in revised form 18 March 2003

Abstract

Velocity measurements are reported for three-dimensional laminar separated airflow adjacent to a backward-facing step using two-component laser Doppler velocimeter. The backward-facing step, with a height of $S = 1.0$ cm, is mounted in a rectangular duct that has an upstream height of $h = 0.98$ cm, downstream height of $H = 2$ cm, and a width of $W = 8$ cm. This geometry provides an aspect ratio of $AR = 8$ and an expansion ratio of $ER = 2.02$. The flow measurements covered a Reynolds number range between $98.5 \leqslant Re \leqslant 525$. Measurements of velocity distributions reveal that a swirling "jet-like" flow develops near the sidewall in the separating shear layer, and the impingement of that flow on the stepped wall causes a minimum to develop in the spanwise distribution of the reattachment region. Reverse and recirculation flow regions develop adjacent to both the sidewall and the step, and these regions increase in size as the Reynolds number increases. Velocity distributions that were measured at various planes downstream from the step are presented, and predictions compare favorably with these measurements. The results show some interesting flow behaviors that could not be deduced from two-dimensional studies.

1. Introduction

Measurements in separated and reattached backward-facing step flow have focused on the two-dimensional flow geometry (see, for example [1–4]; and the references cited therein). This geometry is very simple, yet the flow through it contains most of the complexities that are encountered in other separated flow geometries, and for that reason it has been used in benchmark studies [5,6]. A considerable knowledge base has been established both numerically and experimentally for this flow using ducts with large aspect ratio, and there is a need to extend this knowledge base to the three-dimensional domain because actual systems exhibit three-dimensional behavior.

Measurements by Armaly et al. [2] demonstrated that the flow downstream of a backward-facing step in a rectangular duct with aspect ratio of 18 remained two-dimensional only for low Reynolds number flow and at higher Reynolds numbers three-dimensional effects become significant near the sidewalls. Similarly, measurements by Papadopoulos and Otugen [7] demonstrated that the aspect ratio has a significant influence on both the velocity and the wall pressure distributions even for ducts with relatively large aspect ratio. Numerical simulations by Iwai et al. [8] demonstrated that an aspect ratio greater than 16 is needed to maintain a small two-dimensional region near the centerline of the duct at Reynolds number of 250 (Reynolds number based on step height S and average inlet velocity u_0), and for higher Reynolds number the three-dimensional effects become significant throughout the duct. Numerical simulations by Chiang and Sheu [9] revealed the developments of a sidewall recirculation flow region in three-dimensional backward-facing step flow, and Armaly et al. [10] described the swirling "jet-like" flow that develops near the sidewall in the separated shear layer in this geometry. The strong spanwise flow that develops adjacent to the stepped wall makes the use of the two-dimensional definition for identifying the reattachment region inappropriate for the three-dimensional

* Corresponding author. Tel.: +1-573-341-4601; fax: +1-573-341-4607.
E-mail address: armaly@umr.edu (B.F. Armaly).

0017-9310/03/$ - see front matter © 2003 Elsevier Ltd. All rights reserved.
doi:10.1016/S0017-9310(03)00153-4

Nomenclature

AR	aspect ratio $= W/S$
ER	expansion ratio $= H/h$
H	duct height downstream of the step
h	duct height upstream of the step
L	half width of the duct
Re	Reynolds number $= 2\rho u_0 h/\mu$
S	step height
u	velocity component in the x-direction
u_0	average inlet velocity
v	velocity component in the y-direction
W	width of the duct
w	velocity component in the z-direction
x	streamwise coordinate axis
x_u	locations where the streamwise velocity component (u) is zero
y	transverse coordinate axis
z	spanwise coordinate axis

Greek symbols

μ	dynamic viscosity
ρ	density

separated flow case, as noted by Nie and Armaly [11]. Numerical simulations of three-dimensional separated flow have brought to light some of the complicated flow features that develop in a small aspect ratio duct with backward-facing step, but measurements of such behavior have not appeared in the literature.

Measurements in three-dimensional separated flow have been limited to only a few specific studies. Lim et al. [12] reported on measurements of turbulent, incompressible flow adjacent to a backward-facing step in a duct with a very small aspect ratio, and found that the reattachment length was considerably shorter than its equivalent in two-dimensional backward-facing step flow. Shih and Ho [13] reported limited results for three-dimensional recirculation flow in a tunnel with an aspect ratio of 3 and an expansion ratio of 2.7 using a one-component laser Doppler velocimeter (LDV) system. Papadopoulos and Otugen [7] examined the effects of aspect ratio on the turbulent flow characteristics using a hot wire probe, and only the velocity at the center of the tunnel was reported. To the best of the authors' knowledge, measurements of velocity distributions in three-dimensional separated backward-facing step flow have not been reported in the literature. Such data are needed to validate existing flow simulation codes, and that need motivated the present study.

2. Experimental apparatus and procedures

A schematic of the open-air tunnel that was used in this study is shown in Fig. 1. The tunnel was constructed by using Plexiglas sheets (0.95 cm thick) that are machined and assembled to form the desired geometry. The two sidewalls of the test section were made of optical glass (0.6 cm thick) in order to facilitate flow visualizations and LDV measurements. The upstream portion of the air tunnel has a cross section of 0.98 cm in height (h)

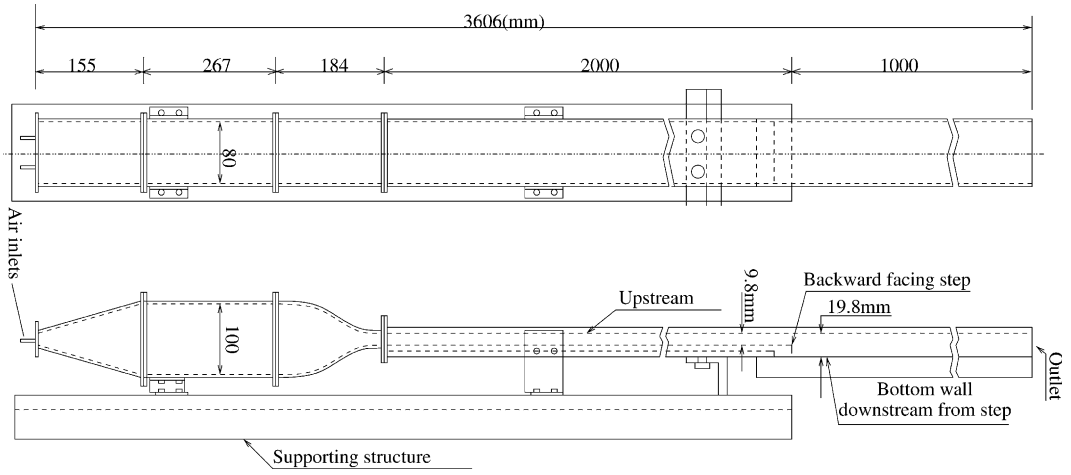

Fig. 1. Schematic of air tunnel (dimension in mm).

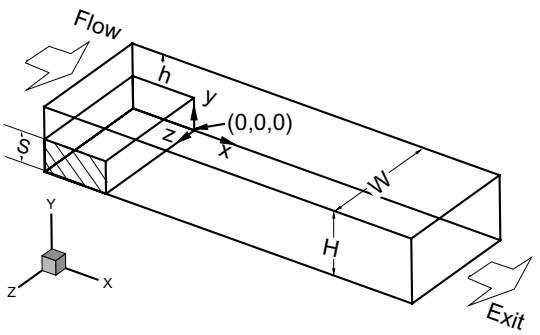

Fig. 2. Schematic of the test section.

and 8.0 cm in width (W), and it is 200.0 cm long. This length is sufficient to ensure fully developed airflow at the step. The downstream portion of the air tunnel has a cross section of 1.98 cm in height (H) and 8.0 cm in width, and it is 100.0 cm long. This length allows the establishment of fully developed flow downstream from the step at the exit section of the tunnel. This geometry provides a backward-facing step of 1.0 cm in height, an expansion ratio of 2.02:1, and an aspect ratio of 8 at the step. A schematic of the experimental geometry and the coordinate axis that are used in this study is shown in Fig. 2. The inlet section of the tunnel consists of a diverging section, a straight section, and a converging section. The diverging section is packed with steel wool, and the straight section is packed with honeycomb materials. The converging section has an area ratio of 10:1 and its smaller cross section connects directly to the upstream segment of the tunnel. This configuration ensures the developments of fully developed, low turbulence airflow at the edge of the backward-facing step. An aluminum frame supports the tunnel in its vertical orientation. The air supplied to the tunnel originates in a large high-pressure air tank and passes through a pressure regulation system that provides a constant airflow rate to the tunnel. A fraction of the inlet airflow is bypassed through six jet atomizers and that air fraction is seeded with olive oil particles having a mean diameter of less than 0.6 μm. The seeded fraction of the airflow is mixed with the unseeded fraction in a large chamber at the inlet of the tunnel, and that mixture forms the seeded air stream that is supplied to the tunnel.

A two-component LDV system, operating in a backscattering mode, was used to measure velocity distributions. The measuring probe volume could be moved to any desired location in the flow field, with an accuracy of 0.01 cm, by a three-dimensional traverse mechanism. The traverse mechanism and the processing of the Doppler signals were controlled by a personal computer. In preparation for the measurements, the LDV and its traverse system were aligned with the tunnel geometry to insure that the traverse system is moving parallel to the tunnel in both the streamwise and the spanwise directions. The airflow rate through the tunnel was then adjusted to a selected value by adjusting valves of the pressure regulator and the flow meter. The seeding density of the flowing air was adjusted by controlling the fraction of the airflow that is bypassed through the atomizers and by selecting the number of atomizers that are used. Flow visualizations were then performed to examine the general nature of the flow at the step and at various locations downstream from the step. A 15-W collimated white light beam, and also a fiber optics laser light sheet were used for flow visualizations. To ensure a steady state and steady flow conditions at the inlet section, the streamwise velocity component (u) was monitored and its distributions in the transverse and spanwise directions were measured upstream of the step at the center of the streamwise plane of $x/S = -2$. After ensuring that these inlet flow measurements are repeatable, measurements were initiated downstream from the step.

Velocity distributions downstream from the step were measured at different streamwise and spanwise locations. Only two of the velocity components (u and v) could be measured by the LDV system. The third velocity component (w) could not be measured due to the limited capabilities of the LDV system. The approximate boundaries of the recirculation flow regions at the stepped wall and also at the sidewall were also measured by locating the points where the mean streamwise velocity component is zero on a plane that is adjacent to these walls. This procedure was repeated for different Reynolds numbers by adjusting the airflow rate. Repeated measurements in the laminar flow regime, i.e. $Re < 600$, established that 512 acceptable LDV samples are sufficient to accurately determine the local mean velocity in the flow domain. To determine the experimental repeatability, measurements were made at three different locations inside the tunnel for a flow with a maximum inlet streamwise u-velocity of 0.52 m/s. The magnitudes of the velocities at the three locations inside the tunnel were different, ranging from low near the sidewalls to high at the center of the duct. At each location, the average velocity components (u and v) were measured repeatedly (12 times) over a relatively short period of time, and 512 valid LDV data points were used to calculate the average velocity for each of the 12 runs at each location. The deviation of any average velocity from the average of the 12 averaged values at any of the three locations was under ± 0.01 m/s for u-velocity component and ± 0.005 m/s for v-velocity component.

3. Results and discussions

Measurements of the spanwise distribution of the mean streamwise velocity component (u) at the step ($x/S = 0$) are presented in Fig. 3(a) for different Reynolds

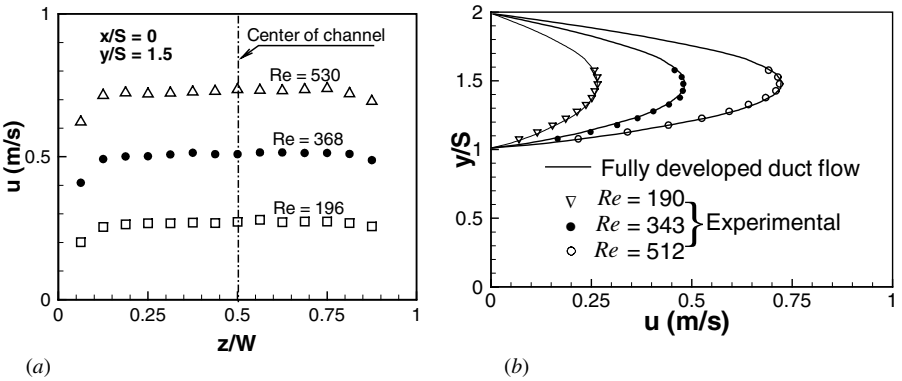

Fig. 3. Distributions of streamwise u-velocity component at the step. (a) Along the spanwise direction at $y/S = 1.5$, (b) along the transverse direction at $z/W = 0.5$.

numbers. These measurements were taken at the center width of the upstream section of the duct. As can be seen from this figure, the flow at the step is symmetric relative to the center of the duct's width for the range of velocities presented in this study. In addition, the results in Fig. 3(a) show that the mean streamwise velocity component is uniform in approximately 80% of the duct's spanwise width. The measured transverse distribution of the mean streamwise velocity component at the center of the tunnel's width ($z/W = 0.5$) and at the step ($x/S = 0$) is presented in Fig. 3(b). These measurements show that the flow is close to fully developed and parabolic at the step. The average inlet velocity (u_0) that is used in the definition of the Reynolds number is equal to 0.62 times the measured maximum mean streamwise velocity component (center line velocity) at $x/S = -2$. This is equivalent to the average velocity of fully developed three-dimensional laminar flow in a rectangular duct [14].

The location where the magnitude of the streamwise component of the wall shear stress is zero at the stepped wall was measured (x_u/S), and the results are presented in Fig. 4. The location on the stepped wall where the streamwise component of the wall shear stress ($\mu \partial u/\partial y|_{y=0}$) is equal to zero ($x_u$-line) is normally used to identify the reattachment length for two-dimensional separated flow. This location is determined by locating the region where the mean streamwise velocity component is changing sign from positive to negative (i.e., $u = 0.0$) at a plane that is parallel to and 0.1 cm away from the stepped wall. One to 10 min of measurements, depending on the state of the flow and the location in the flow field, were needed to gather the 512 velocity samples that were used to identify such a location. Repeatability of identifying the location of the x_u-line from these measurements was 0.01 cm. The x_u-lines exhibit strong variations in the spanwise direction, with a minimum that develops near the sidewall. The maximum in each distribution occurs at the sidewall ($z/L = 0$), and the minimum occurs at approximately $z/L = 0.25$. The region between the step and the x_u-line (equivalent to the recirculation region in two-dimensional flow) increases in size, and its spanwise variation increases with increasing Reynolds number. Predicted results compare favorably with measured values. It is important to note that the x_u-line is not equivalent to either the reattachment line or the outer edge of the recirculation region in this three-dimensional flow. The strong spanwise flow that develops adjacent to the stepped wall in that region makes it very difficult to measure or define from numerical simulation a reattachment line [11]. The numerically predicted results are developed from solving the steady laminar three-dimensional Navier–Stokes equations together with the continuity equation, using finite difference scheme. Hexahedron volume elements and non-uniform staggered grid arrangement are employed in the simulation. SIMPLE algorithm is utilized for the pressure correction in the iteration procedure. The resulting finite difference equations are solved numerically by making use of a line-by-line method combined with ADI scheme. The grid is highly concentrated close to the step and near the corners, in order to insure the accuracy of the numerical simulation. Descriptions and details of the numerical simulation and its convergence, along with the general flow features that develop in this flow geometry, can be found in Nie and Armaly [11].

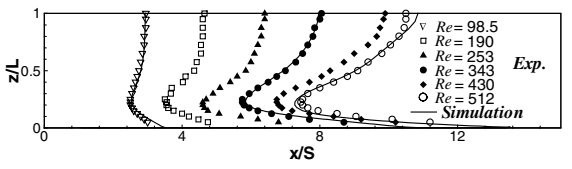

Fig. 4. Distributions of x_u-lines adjacent to the stepped wall ($y = 0.1$ cm).

The negative pressure gradient that develops in the flow due to the sudden expansion, and the jet-like flow that develops in the separating shear layer, are responsible for the reverse flow region that develops adjacent to the sidewall [10,11]. An attempt was made to quantify the flow and the size of this region. A thin laser light sheet was used to visualize the flow adjacent to the upper corner of the sidewall, and from these observations it was determined that for $Re \leqslant 98.5$ there was no recirculation flow region adjacent to the sidewall. At a Reynolds number of 190 ($Re = 190$), a small recirculation flow region was detected in the upper corner of the sidewall. This sidewall recirculation flow region increases in size (length, width, and depth) as the Reynolds number increases. Laser-Doppler measurements were used to determine the locations (x_u-line) where the magnitude of the mean streamwise velocity component is zero on a plane that is parallel to and 0.2 cm away from the sidewall ($z = 0.2$ cm). The procedure used for locating the x_u-line adjacent to the sidewall is similar to the one described above for locating the x_u-line on the stepped wall. The results that are presented in Fig. 5 show that the size of the sidewall recirculation flow region increases with increasing Reynolds number and the predicted values appear to agree very well with the measurements.

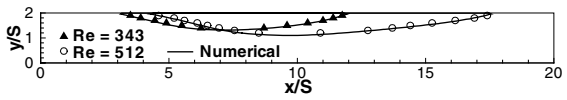

Fig. 5. Distributions of x_u-lines adjacent to the sidewall ($z = 0.2$ cm).

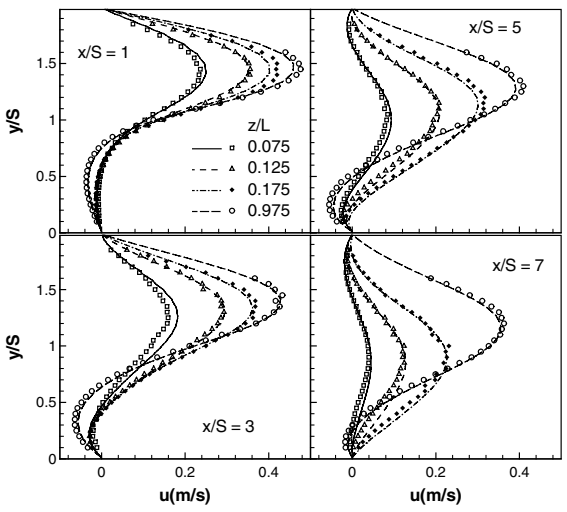

Fig. 6. Transverse distributions of the measured and predicted u-velocity components on different z-planes ($Re = 343$).

Detailed measurements of velocity distributions downstream of the step were performed to determine experimentally the general features of the three-dimensional flow. Transverse distributions of the streamwise velocity component (u) are presented in Fig. 6, for different z-planes for $Re = 343$ at four streamwise locations. These results show clearly the reverse flow region that develops downstream and adjacent to the step at $x/S = 1$, 3, and 5 for all the z-planes that are presented in this figure. For $x/S = 7$, the reverse flow region

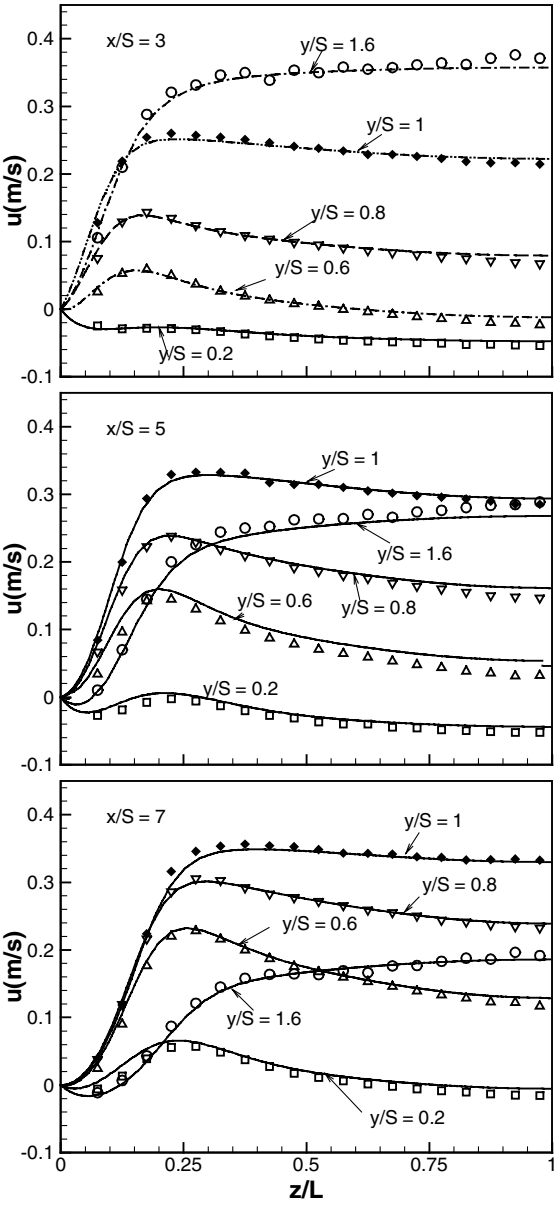

Fig. 7. Spanwise distributions of the measured and predicted u-velocity components on different y-planes ($Re = 343$).

downstream from the step appears only at planes $z/L = 0.075$ and 0.975. The velocity profiles at the other two planes of $z/L = 0.125$ and 0.175 at $x/S = 7$ do not show any reverse flow, because a minimum in the x_u-line develops in that region and the flow at these sections is downstream of the x_u-line. This can also be seen from the results that are presented for the x_u-line in Fig. 4. The results in Fig. 6 also show the developments of the reverse flow region near the upper corner of the sidewall for $z/L = 0.075$ at $x/S = 5$ and for $z/L = 0.075$, 0.125, and 0.175 at $x/S = 7$. Spanwise distributions of the same velocity component for different y-planes are presented in Fig. 7 for different streamwise x-locations. These distributions clearly show the development of a maximum (peak) in that velocity component at approximately $z/L = 0.25$ at y-planes below the step. The development of this peak in the spanwise distribution of this velocity component can also be seen in Fig. 8, where it is presented for different x locations at different y-planes. The peak appears in these distributions only for planes below the step height ($y/S < 1$), and the spanwise location of that peak moves toward the center of the duct as the streamwise distance from the step (x) increases. These distributions show that a jet-like flow (peak in the streamwise velocity distribution) develops adjacent to the sidewall. The impingement of the jet-like flow on the stepped wall is responsible for the minimum that appears in the x_u-line. The reverse flow region that develops at the upper corner of the sidewall can also be seen in Fig. 7 for $y/S = 1.6$ at $x/S = 5$ and 7. The predicted results compare favorably with measured values of the streamwise velocity components as shown in these figures.

Measured and predicted transverse distributions of the transverse velocity component (v) for different z-planes are presented in Fig. 9 at different streamwise locations. These results show the general nature of the downward flow that develops as a result of the sudden expansion in this geometry. The results clearly show that the velocity of the downward flow at the center of the duct is smaller than what develops near the sidewall (downward wash near the sidewall). The location where this velocity component is maximum moves toward the center of the duct as the streamwise distance from the step increases, i.e. from $z/L = 0.075$ at $x/S = 1$, to $z/L = 0.125$ at $x/S = 3$, to $z/L = 0.225$ at $x/S = 7$. This can be seen more clearly from the results that are presented in Figs. 10 and 11 where spanwise distributions of the same velocity component are presented for different x- and y-planes. For example, the results in Fig. 10 at

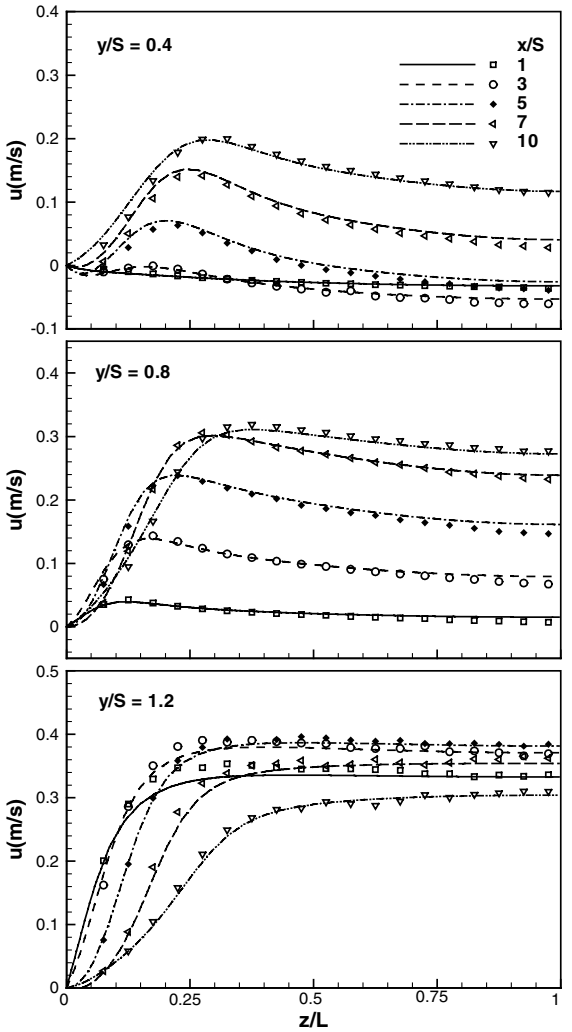

Fig. 8. Spanwise distributions of the measured and predicted u-velocity components on different x-planes ($Re = 343$).

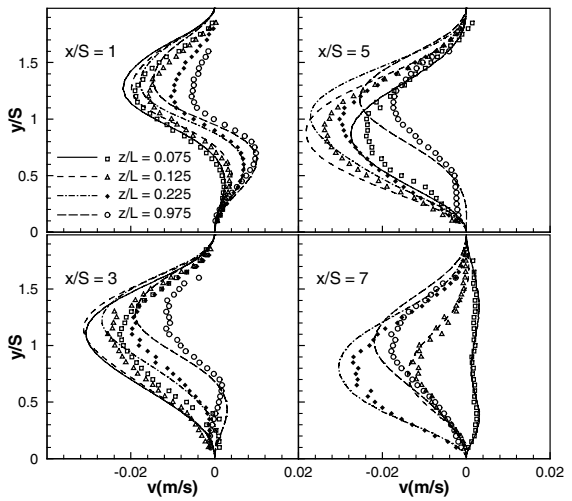

Fig. 9. Transverse distributions of the measured and predicted v-velocity components on different z-planes ($Re = 343$).

$y/S = 0.8$ show that a negative peak develops in that velocity component very close to the sidewall at $x/S = 1$. The magnitude of that peak increases as the streamwise distance increases (i.e. $x/S = 3$ and 5), however, that peak starts to decrease as the downstream distance from the step continues to increase (i.e. $x/S = 7$ and 10). The spanwise location of the velocity peak moves toward the center of the duct as the distance from the step increases. The positive velocity peak that is seen in these distributions near the sidewall is part of the recirculation flow region that develops in this geometry adjacent to the sidewall. The negative velocity peak that develops in these distributions near the sidewall adds to the strength of the jet-like flow that impinges on the stepped wall. The agreement between predicted and measured results is reasonable (not as good as for the streamwise velocity component) considering the small magnitude of that velocity component.

The spanwise w-velocity component could not be measured by the two-component LDV system, but predicted results for that component are presented in Figs. 12–14 in order to provide a more complete picture of the flow behavior. The results in Fig. 12 illustrate some transverse distributions of that velocity component. The results that are presented for planes of $x/S = 3$ and 5 (planes located upstream of the x_u-line and inside the primary recirculation region) illustrate the significant

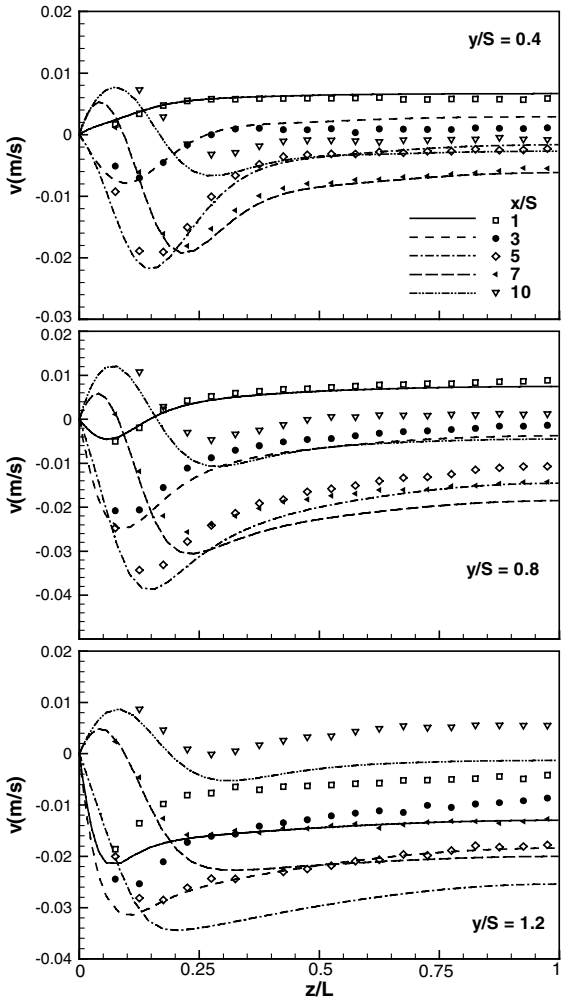

Fig. 10. Spanwise distributions of the measured and predicted v-velocity components on different x-planes ($Re = 343$).

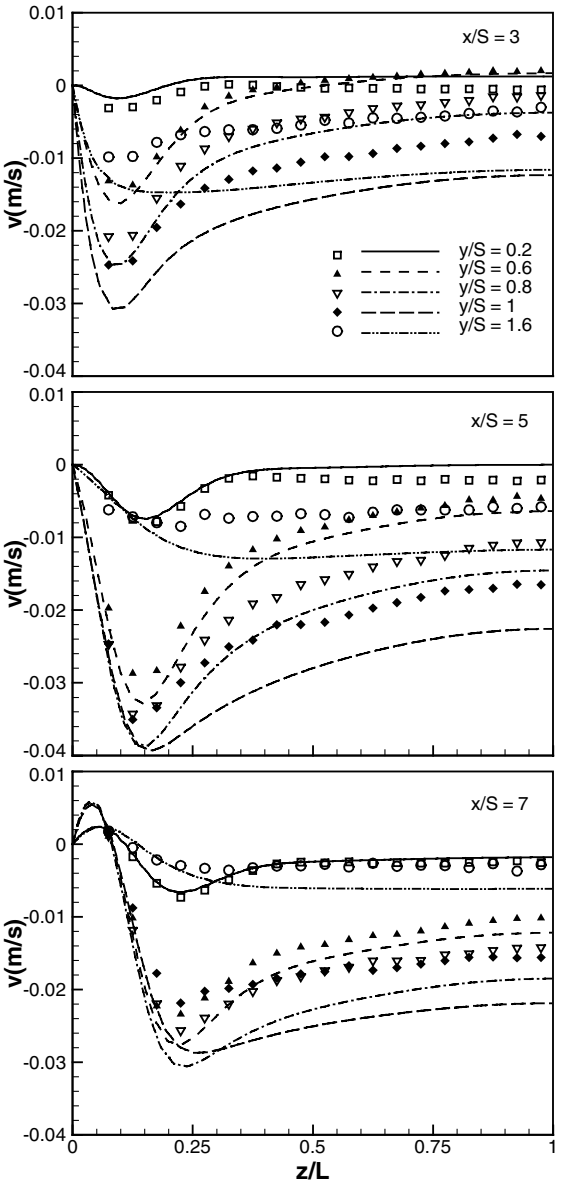

Fig. 11. Spanwise distributions of the measured and predicted v-velocity components on different y-planes ($Re = 343$).

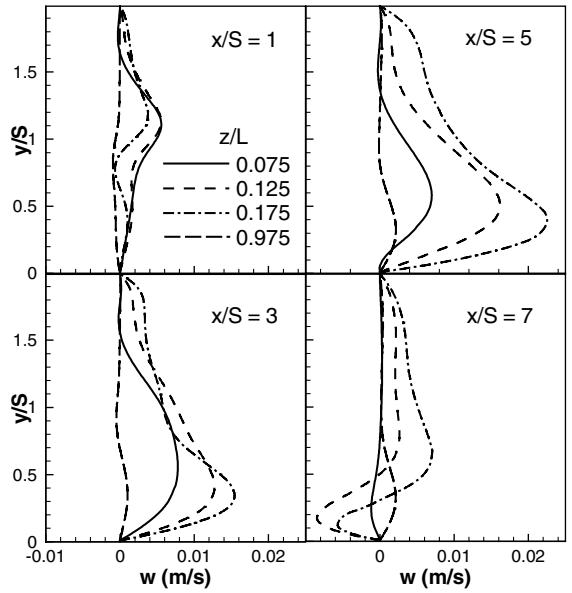

Fig. 12. Transverse distributions of the predicted w-velocity component on different z-planes ($Re = 343$).

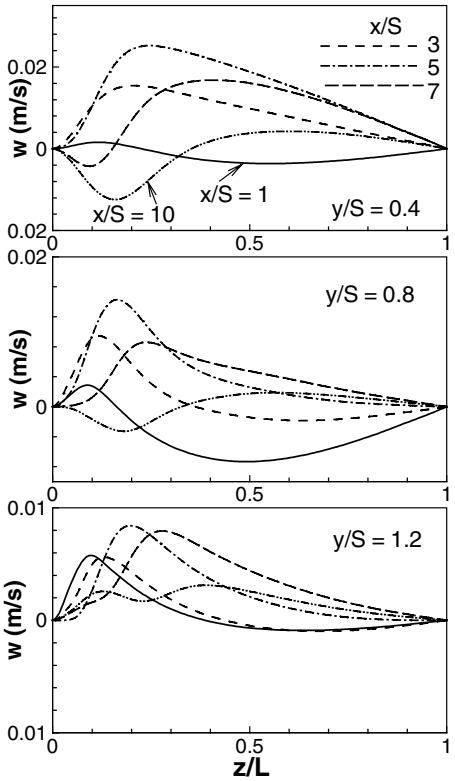

Fig. 13. Spanwise distributions of the predicted w-velocity component on different x-planes ($Re = 343$).

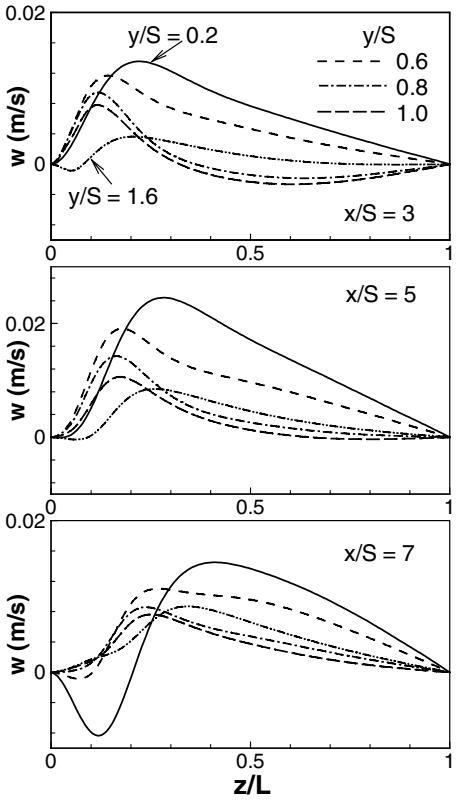

Fig. 14. Spanwise distributions of the predicted w-velocity component on different y-planes ($Re = 343$).

magnitude of spanwise velocity component that develops in the neighborhood of the reattachment region. The counterclockwise swirling flow that develops downstream from the step and adjacent to the stepped wall moves toward the center width of the duct. The negative spanwise velocity component that can be seen in that figure at the plane of $x/S = 7$, indicates that part of the jet-like flow that impinges on the stepped wall flows toward the sidewall and feeds the developing sidewall recirculation flow region. The results in Fig. 13 show that the highest positive value (flow toward the center of the duct) for this component (in the range of the results presented) appears at $y/S = 0.4$, $x/S = 5$, $z/S = 0.25$, and the highest negative value (flow towards the sidewall) appears at $y/S = 0.4, x/S = 10, z/S = 0.12$. Similar results can be seen in Fig. 14 where spanwise distributions of that velocity component are presented for different y-planes at different streamwise locations. The spanwise w-velocity component adjacent to the stepped wall starts at zero at the impingement point of the jet-like flow (a source) and increases sharply in all directions (see [11]) reaching a maximum before starting to decrease to zero as it approaches the sidewall or the center of the duct.

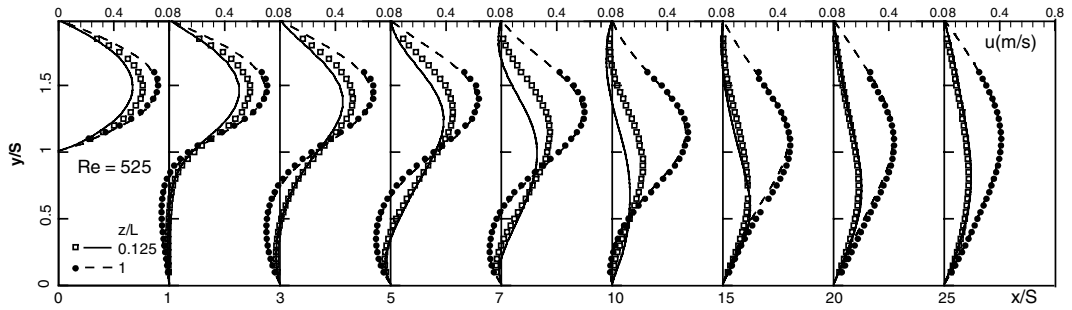

Fig. 15. Measured and predicted transverse distributions of u-velocity component for $Re = 525$ at different x/S and z/L planes.

Comparisons between predicted and measured streamwise velocity component for $Re = 525$ at two spanwise planes, $z/L = 0.125$ and 1, are presented in Fig. 15. Similar flow behavior can be observed for the two spanwise planes that are presented in this figure, with the flow at $z/L = 0.125$ showing the recirculation flow region that develops near the sidewall and the flow at $z/L = 1$ showing the recirculation flow region that develops adjacent to the step. The agreement between the predicted and measured values at $z/L = 1$ is very good, but larger deviations appear to exist for $z/L = 0.125$ due to the small magnitude of the velocity and the difficulties that are associated with the measurements close to the wall.

4. Conclusions

Measurements (using LDV) of the streamwise and transverse velocity components (u and v) in three-dimensional laminar separated flow adjacent to backward-facing step are presented and compared with predictions. Recirculation flow regions develop adjacent to the sidewall and the stepped wall. The streamwise velocity component in the separating shear layer exhibits a peak in its spanwise distribution near the sidewall, thus forming a jet-like flow that impinges on the stepped wall. This jet-like flow is responsible for the minimum that develops in the spanwise distribution of the x_u-line on the stepped wall (a line that locates the position where the streamwise component of the wall shear stress is equal to zero). The size of the recirculation region adjacent to the step and adjacent to the sidewall increases with increasing Reynolds number. The maximum of the x_u-line at the stepped wall for a fixed Reynolds number occurs at the sidewall and not at the center of the duct, as one may expect. A strong spanwise velocity component in both positive and negative directions develops adjacent to the stepped wall, making it difficult to define a specific location for the reattachment region for this separated flow. The definition that has been used to locate the reattachment in two-dimensional separated flow cannot be used for three-dimensional separated flow. Predictions appear to compare very favorably with measurements for most of the reported results.

Acknowledgements

This work was supported in part by the National Science Foundation (NSF) under grants No. CTS-9906746, and CTS-9818203.

References

[1] J.K. Eaton, J.P. Johnson, A review of research on subsonic turbulent flow reattachment, AIAA J. 19 (1981) 1093–1100.
[2] B.F. Armaly, F. Durst, J.C.F. Pereira, B. Schonung, Experimental and theoretical investigation of backward-facing step flow, J. Fluid Mech. 127 (1983) 473–496.
[3] H.I. Abu-Mulaweh, B.F. Armaly, T.S. Chen, Measurements of laminar mixed convection in boundary-layer flow over horizontal and inclined backward-facing steps, Int. J. Heat Mass Transfer 36 (1993) 1883–1895.
[4] S. Jovic, D.M. Driver, Backward-facing step measurements at low Reynolds number, $Re_h = 5000$, NASA Technical Memorandum 108807, NASA, 1994.
[5] B.F. Blackwell, D.W. Pepper, Benchmark Problems for Heat Transfer Codes, ASME HTD, vol. 222, ASME, New York, 1992.
[6] B.F. Blackwell, B.F. Armaly, Computational Aspects of Heat Transfer—Benchmark Problems, ASME HTD, vol. 258, ASME, New York, 1993.
[7] G. Papadopoulos, M.V. Otugen, Separating and reattaching flow structure in a suddenly expanding rectangular duct, Trans. ASME, J. Fluids Eng. 117 (1995) 17–23.
[8] H. Iwai, K. Nakabe, K. Suzuki, Flow and heat transfer characteristics of backward-facing step laminar flow in a rectangular duct, Int. J. Heat Mass Transfer 43 (2000) 457–471.
[9] T.P. Chiang, T.W.H. Sheu, Vortical flow over a three-dimensional backward-facing step, Numer. Heat Transfer—Part A 31 (1997) 167–192.
[10] B.F. Armaly, A. Li, J.H. Nie, Three-dimensional forced convection flow adjacent to backward-facing step, J. Thermophys. Heat Transfer 16 (2002) 222–227.
[11] J.H. Nie, B.F. Armaly, Reattachment of three-dimensional flow adjacent to backward-facing step, in: Proceedings of

8th AIAA/ASME Joint Thermophysics and Heat Transfer Conference, St. Louis, MO, 2002, AIAA-Paper-3013.

[12] K.S. Lim, S.O. Park, H.S. Shim, A low aspect ratio backward-facing step flow, Exp. Thermal Fluid Sci. 3 (1990) 508–514.

[13] C. Shih, C.M. Ho, Three-dimensional recirculation flow in a backward facing step, Trans. ASME, J. Fluids Eng. 116 (1994) 228–232.

[14] R.K. Shah, A.L. London, Laminar Forced Convection in Ducts, Academic Press, New York, 1978.